Analyst

RSC Publishing

PAPER

View Article Online
View Journal | View Issue

Cite this: *Analyst*, 2013, **138**, 5296

A simple green route to prepare stable silver nanoparticles with pear juice and a new selective colorimetric method for detection of cysteine†

Jing Tao Huang,[ab] Xiao Xi Yang,[a] Qiao Ling Zeng[a] and Jian Wang*[a]

Received 2nd May 2013
Accepted 27th June 2013

DOI: 10.1039/c3an00901g

www.rsc.org/analyst

In this work, a new cost-effective, rapid and simple method for the preparation of stable silver nanoparticles (AgNPs) was developed, which can be completed within 15 minutes at room temperature by oxidizing the reductants in pear juice with $AgNO_3$. Compared with the most used citrate-capped AgNPs, the as-prepared AgNPs showed high stability, good biocompatibility and enhanced antibacterial activity. Based on the formation of Ag–S covalent bonds between cysteine and AgNPs as well as the electrostatic interaction of COO^- and NH_4^+ between cysteine molecules, which selectively lead to the aggregation of the as-prepared AgNPs and give a specific yellow-to-red colour change, a new selective colorimetric method for detection of cysteine was proposed with the as-prepared AgNPs by coupling the decrease of the characteristic localized surface plasmon resonance (LSPR) absorption at 406 nm of the as-prepared AgNPs and the increase of the new aggregation-induced band at 530 nm. The ratio of the absorbance at 530 nm to 406 nm (A_{530}/A_{406}) was found to be linearly dependent on the cysteine concentrations in the range of 5.0×10^{-7} to 1.0×10^{-5} M with a limit of detection of 6.8×10^{-8} M.

Introduction

Metal nanomaterials have attracted much attention owing to their unique properties and wide applications in biosensing,[1,2] catalysis,[3] cellular imaging,[4] cancer clinical diagnosis[5] and therapy.[6] With considerable efforts made for the synthesis of metal nanomaterials, several strategies have been reported in the literature for their preparation, including wet chemical preparation,[7] photochemical synthesis[8] and electrochemical method,[9] but the most commonly used is the wet chemical method, in which chemical reducing reagents were employed such as citrate,[10] hydroxylamine hydrochloride,[11] and $NaBH_4$.[12] The above-mentioned preparation methods, however, suffer from significant drawbacks. For example, most methods generally produced unstable nanoparticles and thus surfactants were used.[13,14] The problem is that it might introduce certain unfavourable cytotoxic surfactants.[15] In addition, time-consuming or severe preparation conditions render them difficult to generalize.[16] The challenge is thus to develop new strategies to improve the synthetic procedures.

In order to overcome above-mentioned shortcomings, natural products, such as banana peel, citrus fruits and papaya fruits,[17–20] have been employed to prepare nanoparticles through redox reactions since such reducing reagents as ascorbic acid, phenolic compounds, and sugars are abundant in these fruits. The proteins in the fruits could stabilize the resultant nanoparticles.[18] Despite the aforementioned improvements, however, disadvantages such as time-consuming nature[20] or severe synthetic conditions persist as well.[21] For example, Kothari *et al.* synthesized silver nanoparticles (AgNPs) using a papaya fruit extract, paving a new green way for the preparation of nanoparticles, but it required up to five hours of reaction time at room temperature.[20] Zinjarde *et al.* prepared gold nanoparticles (AuNPs) with banana peel, which could be accomplished in a short time but the protocol demands high temperature.[21] Therefore, developing simple and rapid synthetic methods for nanomaterials using natural products would still be desirable.

In this work, we demonstrate a simple, rapid and green preparative strategy toward stable AgNPs by reducing $AgNO_3$ with pear juice (displayed in Scheme 1) under alkaline conditions, which can be completed within 15 minutes at room temperature. Compared with previously reported methods, the one reported herein is both cost-effective and eco-friendly, obviating the use of any surfactants or lengthy protocols. One advantage of the synthetic method is that the resultant nanoparticles are highly stable even in strongly salty media, and possess unique

[a]*Education Ministry Key Laboratory on Luminescence and Real-Time Analysis, College of Pharmaceutical Sciences, Southwest University, Chongqing 400715, PR China. E-mail: wj123456@swu.edu.cn; Fax: +86-23-68367257; Tel: +86-23-68254059*

[b]*College of Chemistry and Chemical Engineering, Xiamen University, Xiamen 361005, PR China*

† Electronic supplementary information (ESI) available: The absorption spectrum and SEM imaging of AgNPs reduced by citrate trisodium; the dependence of AgNP synthesis on the concentrations of pear juice and NaOH; effects of concentrations of NaCl and pH on the response of AgNPs to cysteine. See DOI: 10.1039/c3an00901g

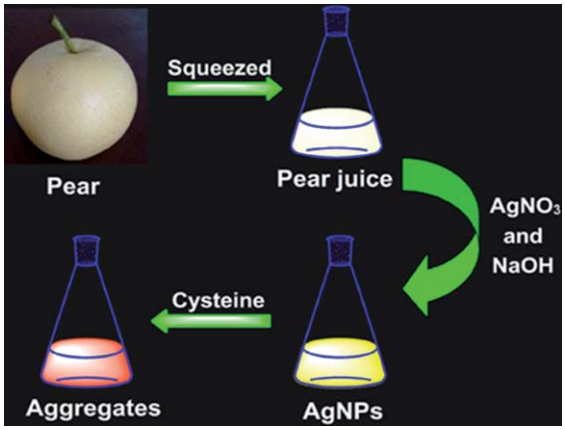

Scheme 1 The simple and green route to preparing AgNPs with pear juice as the colorimetric platform for cysteine detection.

properties of good biocompatibility and enhanced antibacterial activity. Furthermore, the as-prepared AgNPs can be used for selective and colorimetric detection of cysteine in the presence of other common amino acids and glutathione (GSH) through the formation of Ag–S covalent bonds between cysteine and AgNPs as well as the electrostatic interaction between COO^- and NH_3^+ among cysteine molecules.[16]

We chose cysteine as the detecting target because the thiol-containing amino acid plays a crucial role in physiological processes such as detoxification, and metabolism.[22] Besides, cysteine is a potential neurotoxin biomarker for medical conditions and disease-associated physiological regulator,[23] and it provides important insights into the proper physiological functions and diagnosis of diseases. Many diseases such as hematopoiesis, leukocyte loss, and psoriasis may result from the deficiency of cysteine.[24] Therefore, the great significance to sense cysteine is well understood.

Experimental section

Materials

Amino acids including L-alanine (Ala), L-arginine (Arg), L-asparagine monohydrate (Asn), L-cysteine (Cys), L-cystine (cys–cys), L-glycine (Gly), L-histidine (His), L-isoleucine (Ile), L-leucine (Leu), L-lysine (Lys), L-methionine (Met), L-phenylalanine (Phe), L-proline (Pro), L-serine (Ser), L-threonine (Thr), L-tryptophan (Trp), L-tyrosine (Tyr), L-valine (Val) were purchased from Shanghai Kangda Factory of Amino Acid (Shanghai, China). Glutathione (GSH) was obtained from Sigma.

Escherichia coli (ATCC 25922), *Pseudomonas aeruginosa* (ATC27853) and *Staphylococcus aureus* (ATCC 25923) were employed to detect the antibacterial activity of AgNPs, while Hep-2 cancer cells were used for checking the cytotoxicity.

Huangguan pear was purchased from Chongbai Supermarket (Beibei, Chongqing). Sodium hydroxide (NaOH) and silver nitrate ($AgNO_3$) were obtained from Chuandong Chemical Group Co., Ltd. (Chongqing, China) and Ruijinte Chemical Group Co., Ltd. (Tianjin, China), respectively. NaCl and Britton–Robinson (BR) buffer were employed to adjust the ionic strength and control the acidity, respectively.

Instruments

A Hitachi U-3010 spectrometer (Tokyo, Japan) was used to record the absorption spectra of AgNPs and their aggregates. A Hitachi S-4800 scanning electron microscope (SEM, Tokyo, Japan) and a JEOL JEM-2100 transmission electron microscope (TEM, Tokyo, Japan) were used to measure the images of AgNPs, respectively. An E-510 Olympus camera (Tokyo, Japan) was employed to record the colourful pictures. The infrared spectrum was obtained by a Perkin Elmer Spectrum GX Fourier Transform Infrared (FT-IR) spectrometer (MA, USA) in a KBr wafer. X-ray photoelectron spectroscopy (XPS) data were measured by an ESCAlab 250 XPS system with an Al Kα source. A dynamic light scattering (DLS) Nano-zs zetasizer (Malvern, England) was used to estimate the size of AgNPs. Dark-field light scattering photographs of AgNPs on the glass slide were captured with a Nikon 4500 digital camera coupled to the Olympus BX51 dark-field system (Tokyo, Japan). The cell viability was detected with an Epoch microplate spectrophotometer system (BioTek, VT, USA), and bacteria were cultured in a full temperature bacterial racking (Guangzhou, China). pH values were measured with a Cyber Scan pH/Ion 510 digital pH meter (Eutech, USA).

Synthesis of AgNPs using pear juice as the reducing reagent

The Huangguan pear was firstly peeled and the pear flesh was then squeezed to obtain a colourless juice, which was further purified by centrifugation at 10 000 rpm for 5 min to remove the remaining small solids. *It should be noted that the juice would turn brownish in the air easily if stored for more than two hours at room temperature owing to the air oxidation effect, which is not beneficial for later work. To avoid the unfavourable air oxidation effect, a good way to store the pear juice is in a −20 °C refrigerator in an obturator, which could be stable at least for 5 months.* Into 500 μL of the purified pear juice, $AgNO_3$ (500 μL, 10 mM) and NaOH (200 μL, 0.1 M) were added in sequence and mixed. Yellowish brown AgNPs were then produced at room temperature within 15 minutes.

Synthesis of AgNPs using citrate trisodium as the reducing reagent

For comparison purposes, another batch of AgNPs was synthesized using citrate sodium as the reducing reagent according to ref. 25 and 26. Briefly, 50.0 mL of the solution containing 1.0 mM $AgNO_3$ was added into a 100 mL conical flask, and was heated until boiling under continuous stirring, and subsequently, 2.0 mL of 1% (w/w) citrate trisodium was introduced. The colloidal solution was kept boiling for about 30 min under vigorous stirring until it was cooled down to room temperature. The above aqueous mixture gradually changed from brown to yellow, indicating the formation of AgNPs.

Standard procedure for cysteine detection

Into a 1.5 mL plastic vial, 0.10 mL BR buffer (pH 2.56), 0.02 mL AgNPs and an appropriate amount of cysteine were initially mixed. Then, 0.10 mL 1 M NaCl was introduced and vortexed thoroughly. Finally, the mixture was diluted to 0.50 mL with

doubly distilled water and blended again. The absorption spectra were scanned on a U-3010 UV-vis spectrofluorometer from 300 to 800 nm.

Results and discussion

Synthesis of AgNPs

Since pear juice, which contained such reductants as ascorbic acid, phenolic compounds, and sugars, was employed for AgNP synthesis, the contents of these reductants were found to have effects on the synthesis of nanoparticles.[8] In our experiment, the juice was used as obtained and mixed with 0.01 M $AgNO_3$ with the volume ratio varying from 1 : 9 to 9 : 1 (see the ESI, Fig. S1†). When either the concentration of juice or $AgNO_3$ was low, *i.e.* 1 : 9 or 9 : 1, for example, few nanoparticles were obtained. Further experiments showed that when the optimal ratio of juice to $AgNO_3$ was 5 : 5, uniform AgNPs with an average size of 10 nm (see the ESI, Fig. S2†) were formed, which had a narrow characteristic localized surface plasmon resonance (LSPR) absorption band centred at 406 nm (Fig. 1a). Importantly, the sizes of nanoparticles could be regulated by adjusting the ratio of pear juice and $AgNO_3$ (see the ESI, Fig. S3†), and thus AgNPs with the sizes of 50 nm, 30 nm, 10 nm and 7 nm were obtained with the volume ratio varying from 1 : 9, 3 : 7, 5 : 5 to 7 : 3, respectively.

Considering that $AgNO_3$ has strong oxidation capacity under alkaline conditions,[27] a NaOH solution was added to provide high alkalinity to enhance the oxidation capacity of $AgNO_3$. It is worth noting that NaOH serves two other functions: (a) to negatively charge the reductant, which then easily further interacts with silver ions through electrostatic attraction (see the ESI, Fig. S4†); and (b) to prompt the alkaline-responsive mechanism, in which phytochemicals, such as amino acids, organic acids, peptides and/or proteins in the pear juice, may play a role in the formation of nuclei during the reduction of silver ions and their secondary growth.[18] A series of experiments showed that 0.015–0.020 M NaOH was ideal to control the acidity of the mixture of $AgNO_3$ and juice. The pH of the pear juice was about 4.39, but would get increased to 7.52 after the preparation reaction. The near neutral environment supplies the possibility of good biocompatibility for the as-prepared AgNPs.

The synthetic process to prepare AgNPs with pear juice was dynamic although the reaction time was short, during which the size of the resultant AgNPs became smaller and smaller, as shown by the blue-shift of the LSPR band as reduction progressed (Fig. 1b). In comparison, it took more than 1.0 h to obtain AgNPs if citrate trisodium was employed as the reducing reagent according to ref. 25 and 26, indicating that our method was much more efficient.

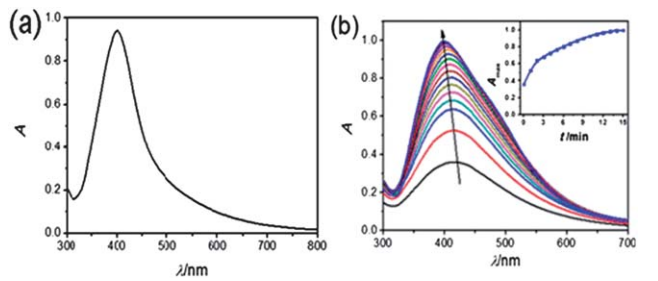

Fig. 1 Formation of AgNPs by reducing $AgNO_3$ with pear juice. (a) The LSPR absorption spectrum of the as-prepared AgNPs; (b) The dynamic process of AgNPs formation.

Characterization of the as-prepared AgNPs

The components of the as-prepared AgNPs were characterized by FTIR spectrum and XPS. As shown in Fig. 2a, the obtained AgNPs exhibited characteristic absorption bands of O–H and N–H stretching vibrations at 3379 cm^{-1}, C–H stretching vibrations at 2935 cm^{-1}, C=O stretching vibrations at 1640 cm^{-1} and C–O–C stretching vibrations at 1060 cm^{-1}, respectively.[28] These functional groups can be ascribed to the degradation of the sugars, peptides or proteins found in pear juice owing to the oxidation of $AgNO_3$ in a NaOH medium.[18]

XPS analysis revealed (Fig. 2b) the existence of carbon, oxygen and nitrogen as well as limited amounts of Na and Ag elements on the surface of AgNPs. Carbon, oxygen and nitrogen mainly came from the sugars, peptides or proteins in the pear juice,[18] while the appearance of Na and Ag elements was due to the introduction of NaOH and $AgNO_3$. It is worth noting that the ratio of nitrogen to Ag is higher than 1 : 1, not identical to that in $AgNO_3$, suggesting that some nitrogen atoms resulted from the pear juice which contained peptides or proteins.[18] Further analysis showed that C–C, C–O, C–N and C=N/C=O groups exist in the C1s spectrum (Fig. 2c),[29] and C=O and C–OH/C–O–C groups in the O1s spectrum (Fig. 2d).[29] The peaks at 367.9 eV and 373.9 eV correspond to the binding energy of $Ag3d_{5/2}$ and $Ag3d_{3/2}$, respectively (see the ESI, Fig. S5†). All these observations indicate that AgNPs were successfully prepared and surrounded with some functional groups coming from sugars, peptides or proteins.[18]

The stability of AgNPs

Retaining high stability is critical in the synthesis of nanomaterials since nanomaterials are prone to aggregation in

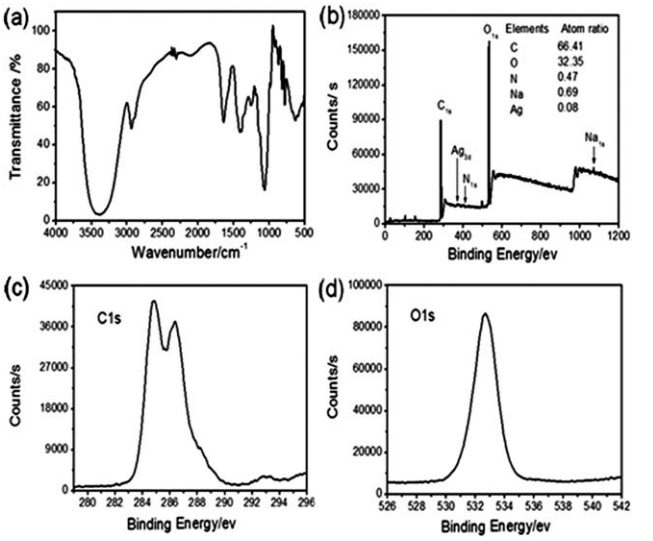

Fig. 2 Characteristics of the as-prepared AgNPs. (a) Fourier transformed infrared spectrum and (b) XPS, (c) C1s and (d) O1s spectra.

highly salty media, thus limiting their applications.[16] As shown in Fig. 3, NaCl exerts strong effects on the citrate-coated AgNPs, and the strong LSPR band at 414 nm greatly decreased in the medium of 0.2 M NaCl with a yellow-to-grey color change (Fig. 3a), indicating the aggregation of AgNPs,[30,31] and suggesting the poor stability of citrate-coated AgNPs in a salty medium. In contrast, the as-prepared AgNPs showed especially high stability, and the LSPR band at 406 nm and the color of the as-prepared AgNPs scarcely changed in the medium of 0.2 M NaCl (Fig. 3b), probably because the alkaline-responsive phytochemicals such as sugars, peptides or proteins surrounded AgNPs to inhibit the aggregation.[18] This high stability supplies the possibility of highly selective detections.

The high stability was further demonstrated in experiments in which the as-synthesized AgNPs were left standing for over seven days. As displayed in Fig. 3c, the LSPR band of the citrate-coated AgNPs decreased by about 20% and the test tube showed a dark silver coating after seven days, which is due to the adsorption of nanoparticles on the walls of the test tubes. By comparison, neither the LSPR absorption band nor the colour in the test tube, however, changed much for the as-prepared AgNPs (Fig. 3d).

The cytotoxicity test and antibacterial activity of the as-prepared AgNPs

The cell viability of Hep-2 cells using a Cell Counting Kit-8 method was used to assess the toxicity of AgNPs (Fig. 4a). AgNPs prepared both with pear juice and citrate did not show obvious cytotoxicity (cell viability $\sim$ 100%), indicating that these nanoparticles are highly biocompatible, allowing the potential use of these nanoparticles in biological applications.

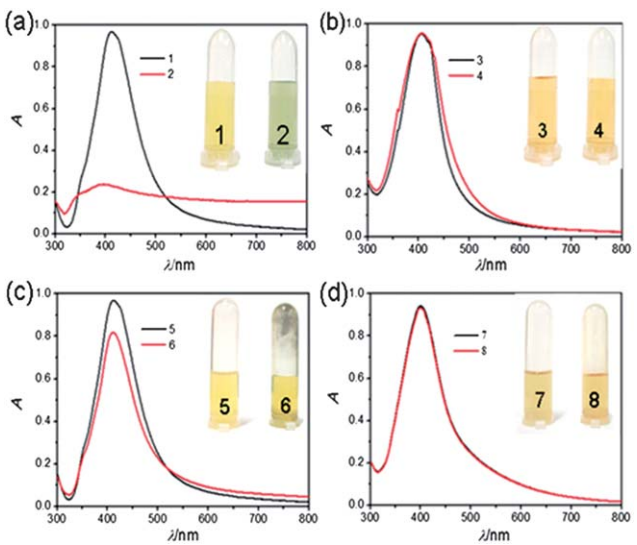

Fig. 3 The stability of AgNPs as tested by the addition of 0.2 M NaCl (a and b) and standing for 7 days (c and d). (a and c) AgNPs prepared by reducing $AgNO_3$ with citrate; (b and d) AgNPs by this method. Concentrations of the as-prepared AgNPs and citrated AgNPs are 2.40×10^{-4} M and 2.08×10^{-4} M, respectively. Dark curves indicate the spectra before the addition of 0.2 M NaCl (curve 1 and 3) or before standing for 7 days (curve 5 and 7), while the red ones indicate those after the addition of 0.2 M NaCl (curve 2 and 4) or after standing for 7 days (curve 6 and 8).

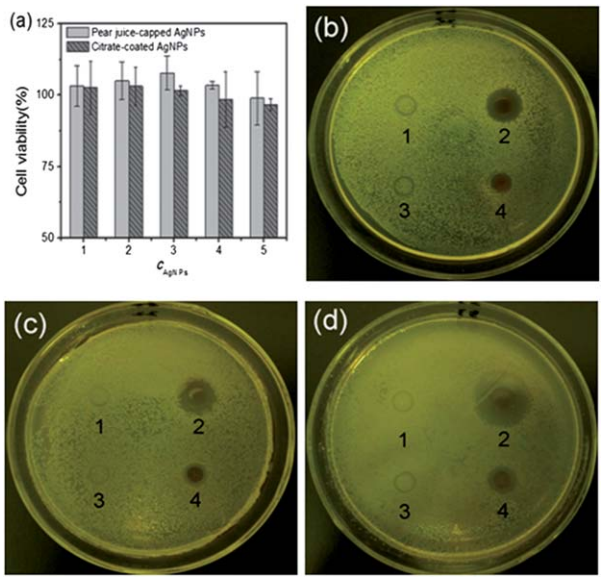

Fig. 4 Cytotoxicity test and antibacterial activity of the as-prepared AgNPs. (a) Cytotoxicity test of AgNPs. c_{AgNPs} (calculated by $AgNO_3$) – 1: 1.0×10^{-9} M; 2: 1.0×10^{-8} M; 3: 1.0×10^{-7} M; 4: 1.0×10^{-6} M; 5: 1.0×10^{-5} M. Antibacterial activity of AgNPs against *Pseudomonas aeruginosa* (b), *Escherichia coli* (c) and *Staphylococcus aureus* (d). 1: pear juice diluted by 10 times; 2: pear juice-coated AgNPs, 1.0×10^{-4} M; 3: citrate trisodium, 0.04% (w/w); 4: citrate-capped AgNPs, 1.0×10^{-4} M.

The antibacterial activity is an important property of AgNPs because AgNPs, Ag^+ ions[32,33] and functionalized AgNPs[34] show excellent antibacterial properties. In this work, the antibacterial activities were demonstrated using a standard Oxford cup method (Fig. 4b–d).[35] Herein, pear juice and citrate were used as the negative control. Indeed, both of them provided ignorable antibacterial results. However, the as-prepared AgNPs with pear juice showed a more significant antimicrobial effect than the citrate-capped AgNPs against *Pseudomonas aeruginosa* (Fig. 4b), *Escherichia coli* (Fig. 4c) and *Staphylococcus aureus* (Fig. 4d), which might be ascribed to the smaller size of the as-prepared AgNPs than that of citrated-coated AgNPs (see the ESI, Fig. S6†).[36] To further confirm this concept, the pear juice prepared AgNPs with different sizes were used to check the antibacterial activities, and it was found that the smallest AgNPs have the strongest antibacterial activity due to the largest values of the inhibition zone (see the ESI, Fig. S7†). The possible reason is that smaller AgNPs are easier to attach onto the cell membrane to change the overall permeability and affect the fundamental functions of the enzymes in the respiratory chain.[36]

The as-prepared AgNPs for cysteine detection

The as-prepared AgNPs could be further applied to cysteine detection. Fig. 5a shows that the LSPR band of AgNPs at 406 nm decreased and a new band at 530 nm emerged with the addition of cysteine, owing to the aggregations of the as-prepared AgNPs through the electric dipole–dipole interaction and coupling between the neighbouring particles.[30,31] To confirm the formation of aggregates, DLS was employed to examine the size

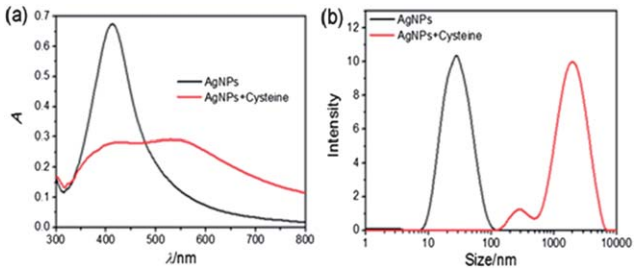

Fig. 5 As-prepared AgNPs used for cysteine detection. (a) Absorption spectra of AgNPs in the absence (dark) and presence (red) of cysteine. (b) Dynamic light scattering (DLS) measurements of AgNPs in the absence (dark) and presence (red) of cysteine. c_{AgNPs}: 1.67 × 10^{-4} M; $c_{Cysteine}$: 8.0 × 10^{-6} M; c_{NaCl}: 0.2 M, pH 2.56.

change of AgNPs. As displayed in Fig. 5b, the mean hydration size of the as-prepared AgNPs was 22 ± 4 nm. With cysteine present, however, the size increased to about 1390 nm, indicating the formation of nanoparticle aggregates.

SEM and dark-field light scattering images were captured to identify the cysteine-induced aggregation. In Fig. 6a, AgNPs were well dispersed but the interparticle distance of AgNPs decreased when cysteine was present, which demonstrated the formation of the Ag–S bond as well as the electrostatic interaction (Fig. 6b).[16] Similarly, the dark-field light scattering images (Fig. 6c and d) also identified the cysteine-induced aggregation of AgNPs. The dispersed AgNPs display green and cyan light scattering,[37] but changed to yellow with the addition of cysteine thanks to the cysteine-induced aggregation.[38]

Ionic strength of the solution exerts strong effects on the cysteine-induced aggregation of AgNPs. The as-prepared AgNPs can effectively withstand the effects of salt (Fig. 3 and ESI, Fig. S8a†) even in a medium of 0.2 M NaCl, but cysteine-induced aggregation of AgNPs was not possible without NaCl even if the aggregation could occur to some degree. The dependence of the cysteine-induced aggregation of AgNPs on the ionic strength might be attributed to the strong electrostatic repulsion among AgNPs, which could be weakened with the addition of NaCl and then improve the formation of the Ag–S covalent bond as well as the electrostatic interaction between COO^- and NH_4^+.[16,39,40] The absorbance ratio (A_{530}/A_{406}) of the cysteine–AgNP aggregates was greatly enhanced on increasing the NaCl concentration to 0.2 M.

In addition to ionic strength, the acidity of the medium has strong influence on the aggregation of AgNPs as well. As stated above, AgNPs synthesized under alkaline conditions might be unstable in acidic media due to the neutralization interaction of the functional groups on the surfaces of the as-prepared AgNPs. Experiments showed that only in media with pH values higher than 2.56 (ESI, Fig. S8b†), the as-prepared AgNPs were well dispersed. In the presence of cysteine, however, AgNP aggregation occurred in a medium with pH values lower than 4.5, and the most efficient cysteine-induced aggregation occurred at pH 2.56.

Sensitivity and selectivity of cysteine detection

Fig. 5a shows that the LSPR band of AgNPs at 406 nm decreased upon the addition of cysteine with the emergence and increase of a new absorption band at 530 nm. With this decrease–increase change, a linear relationship between the ratio of A_{530}/A_{406} and the content of cysteine in a range of 5.0 × 10^{-7} to

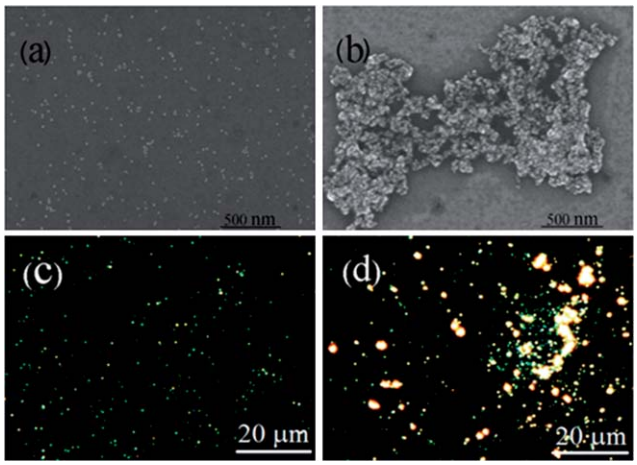

Fig. 6 SEM (a and b) and dark-field light scattering (c and d) images of the as-prepared AgNPs in the absence (a and c) and presence (b and d) of cysteine. Scale bar of (a) and (b): 500 nm; (c) and (d): 20 μm. Exposure time: 0.4 s. c_{AgNPs}: 1.67 × 10^{-4} M; $c_{Cysteine}$: 8.0 × 10^{-6} M; c_{NaCl}: 0.2 M, pH 2.56.

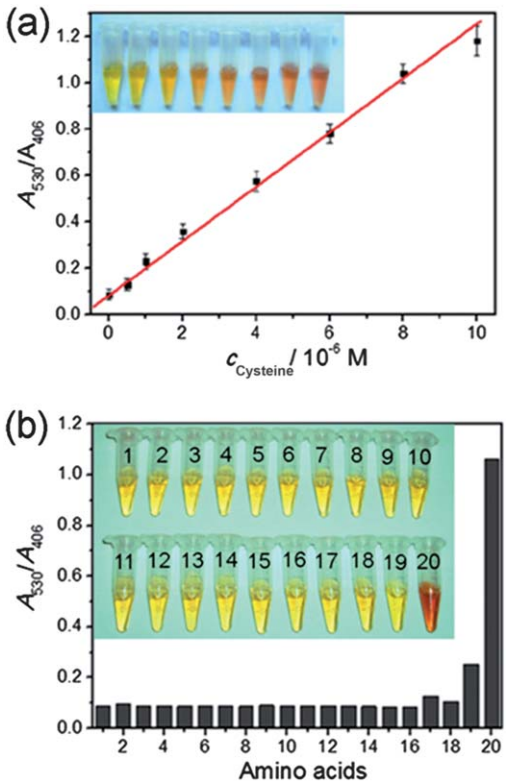

Fig. 7 Detection of cysteine with the as-prepared AgNPs. (a) Calibrated curve for cysteine detection and the corresponding visual images. c_{AgNPs}: 1.67 × 10^{-4} M; c_{NaCl}: 0.2 M, pH 2.56. (b) Selectivity for cysteine detection. c_{AgNPs}: 1.67 × 10^{-4} M; c_{NaCl}: 0.2 M, pH 2.56. 1: control; 2: Ala; 3: Arg; 4: Asn; 5: His; 6: Gly; 7: Cys–cys; 8: Ile; 9: Leu; 10: Lys; 11: Met; 12: Phe; 13: Pro; 14: Ser; 15: Thr; 16: Trp; 17: Tyr; 18: Val; 19: GSH; 20: Cys. c_{AgNPs}: 1.67 × 10^{-4} M; c_{NaCl}: 0.2 M, pH 2.56. All concentrations of amino acids and GSH were 8.0 × 10^{-6} M.

1.0×10^{-5} M could be established (Fig. 7a), which was expressed as $A_{530}/A_{406} = 0.095 + 0.12c$ (1.0×10^{-6} M, $r^2 = 0.9943$) with a limit of detection of 6.8×10^{-8} M (3σ). Consistent with the decrease–increase relationship following the addition of cysteine was the colour change of AgNPs from yellow to red, which supplies a colorimetric assay for cysteine detection.

The cysteine-induced aggregation of AgNPs is highly specific. As Fig. 7b shows, the A_{530}/A_{406} change of AgNPs caused by cysteine is extraordinarily obvious compared with those of other amino acids, indicating that the significant change of absorption in essence is due to the Ag–S covalent bond between AgNPs and thiol group of cysteine as well as COO^- and NH_4^+ electrostatic interaction among cysteine molecules.[31] However, the A_{530}/A_{406} ratios in the cases of cystine (cys–cys) and methionine were relatively weak, even with the –S–S– or –S– groups respectively. Interestingly, GSH, which contains the SH– group, also showed a weak signal owing to the specific steric hindrance.[41] Therefore, the proposed AgNPs showed high selectivity toward cysteine determination.

Conclusions

In summary, we proposed a rapid and simple green synthetic method of AgNPs using pear juice as the reducing reagent, which was cost-effective and biocompatible. The as-prepared AgNPs showed unique properties such as high stability, good biocompatibility and enhanced antibacterial activity, supplying the potential for wide applications. As a proof of concept, a new detection method of cysteine was developed with the as-prepared AgNPs through cysteine-induced aggregation, which occurs owing to the Ag–S covalent bond between AgNPs and thiol group of cysteine as well as COO^- and NH_4^+ electrostatic interaction between cysteine molecules. The highly specific cysteine-induced aggregation of the as-prepared nanoparticles furnishes a new idea to couple thiol-modified DNA, which may also be a feasible approach for DNA detection or other DNA-based biorecognition.

Acknowledgements

All authors herein are grateful to the financial support from the Natural Science Foundation Project of China SWU (SWU112092) and the Fundamental Research Funds for the Central Universities (XDJK2013C159).

Notes and references

1 J. Wang, P. Zhang, J. Y. Li, L. Q. Chen, C. Z. Huang and Y. F. Li, *Analyst*, 2010, **135**, 2826.
2 Y. Liu and C. Z. Huang, *Analyst*, 2012, **137**, 3434.
3 W. Li, J. Li, W. Qiang, J.-J. Xu and D. Xu, *Analyst*, 2013, **138**, 760.
4 L. Q. Chen, S. J. Xiao, L. Peng, T. Wu, J. Ling, Y. F. Li and C. Z. Huang, *J. Phys. Chem. B*, 2010, **114**, 3655.
5 I. Brigger, C. Dubernet and P. Couvreur, *Adv. Drug Delivery Rev.*, 2002, **54**, 631.
6 J. Wang, G. Zhu, M. You, E. Song, M. I. Shukoor, K. Zhang, M. O. D. Altman, Y. Chen, Z. Zhu, C. Z. Huang and W. Tan, *ACS Nano*, 2012, **6**, 5070.
7 N. R. Jana, L. Gearheart and C. J. Murphy, *Chem. Commun.*, 2001, 617.
8 Y. Zhang, X. Yuan, Y. Wang and Y. Chen, *J. Mater. Chem.*, 2012, **22**, 7245.
9 M. Zhou, S. H. Chen, S. Y. Zhao and H. Y. Ma, *Physica E*, 2006, **33**, 28.
10 S. Chen, Y.-M. Fang, Q. Xiao, J. Li, S.-B. Li, H.-J. Chen, H. H. Yang and J.-J. Sun, *Analyst*, 2012, **137**, 2021.
11 S. Kundu, S. Lau and H. Liang, *J. Phys. Chem. C*, 2009, **113**, 5150.
12 Z. Chen, X. Zhang, H. Cao and Y. Huang, *Analyst*, 2013, **138**, 2343.
13 P. Christian and M. Bromfield, *J. Mater. Chem.*, 2010, **20**, 1135.
14 A. V. Singh, B. M. Bandgar, M. Kasture, B. L. V. Prasad and M. Sastry, *J. Mater. Chem.*, 2005, **15**, 5115.
15 A. M. Alkilany, P. K. Nagaria, C. R. Hexel, T. J. Shaw, C. J. Murphy and M. D. Wyatt, *Small*, 2009, **5**, 701.
16 J. Wang, Y. F. Li, C. Z. Huang and T. Wu, *Anal. Chim. Acta*, 2008, **626**, 37.
17 M. V. Sujitha and S. Kannan, *Spectrochim. Acta, Part A*, 2013, **102**, 15.
18 G. S. Ghodake, N. G. Deshpande, Y. P. Lee and E. S. Jin, *Colloids Surf., B*, 2010, **75**, 584.
19 B. Ankamwar, C. Damle, A. Ahmad and M. Sastry, *J. Nanosci. Nanotechnol.*, 2005, **5**, 1665.
20 D. Jain, H. K. Daima, S. Kachhwaha and S. L. Kothari, *Dig. J. Nanomater. Bios.*, 2009, **4**, 723.
21 A. Bankar, B. Joshi, A. Ravi Kumar and S. Zinjarde, *Colloids Surf., B*, 2010, **80**, 45.
22 Z. Guan, S. Li, P. B. S. Cheng, N. Zhou, N. Gao and Q.-H. Xu, *ACS Appl. Mater. Interfaces*, 2012, **4**, 5711.
23 J.-S. Lee, P. A. Ulmann, M. S. Han and C. A. Mirkin, *Nano Lett.*, 2008, **8**, 529.
24 H. Huang, X. Liu, T. Hu and P. K. Chu, *Biosens. Bioelectron.*, 2010, **25**, 2078.
25 J. Ling, Y. F. Li and C. Z. Huang, *Anal. Chem.*, 2009, **81**, 1707.
26 P. C. Lee and D. Meisel, *J. Phys. Chem.*, 1982, **86**, 3391.
27 L. P. Wu, Y. F. Li, C. Z. Huang and Q. Zhang, *Anal. Chem.*, 2006, **78**, 5570.
28 C. Zhu, J. Zhai and S. Dong, *Chem. Commun.*, 2012, **48**, 9367.
29 S. Liu, J. Tian, L. Wang, Y. Zhang, X. Qin, Y. Luo, A. M. Asiri, A. O. Al-Youbi and X. Sun, *Adv. Mater.*, 2012, **24**, 2037.
30 A. Ravindran, V. Mani, N. Chandrasekaran and A. Mukherjee, *Talanta*, 2011, **85**, 533.
31 S. Hajizadeh, K. Farhadi, M. Forough and R. Molaei, *Anal. Methods*, 2012, **4**, 1747.
32 M. Mahmoudi and V. Serpooshan, *ACS Nano*, 2012, **6**, 2656.
33 J. Chao, J. Liu, S. Yu, Y. Feng, Z. Tan, R. Liu and Y. Yin, *Anal. Chem.*, 2011, **83**, 6875.
34 E. Amato, Y. A. Diaz-Fernandez, A. Taglietti, P. Pallavicini, L. Pasotti, L. Cucca, C. Milanese, P. Grisoli, C. Dacarro,

J. M. Fernandez-Hechavarria and V. Necchi, *Langmuir*, 2011, **27**, 9165.
35 Y. Liu, W. Ma, W. Liu, C. Li, Y. Liu, X. Jiang and Z. Tang, *J. Mater. Chem.*, 2011, **21**, 19214.
36 V. Dal Lago, L. Franca de Oliveira, K. de Almeida Goncalves, J. Kobarg and M. Borba Cardoso, *J. Mater. Chem.*, 2011, **21**, 12267.
37 Y. Liu, J. Ling and C. Z. Huang, *Chem. Commun.*, 2011, **47**, 8121.
38 S. J. Zhen, Z. Y. Zhang, N. Li, Z. D. Zhang, J. Wang, C. M. Li, L. Zhan, H. L. Zhuang and C. Z. Huang, *Nanotechnology*, 2013, **24**, 055601.
39 Z. P. Li, X. R. Duan, C. H. Liu and B. A. Du, *Anal. Biochem.*, 2006, **351**, 18.
40 J. Wang, D. M. Wang and Y. F. Li, *Chin. Sci. Bull.*, 2011, **56**, 1196.
41 X. Yuan, Y. Tay, X. Dou, Z. Luo, D. T. Leong and J. Xie, *Anal. Chem.*, 2012, **85**, 1913.